Surgical and Radiologic Anatomy (2021) 43:1989–1998
https://doi.org/10.1007/s00276-021-02799-2

ORIGINAL ARTICLE

A comprehensive morphometric analysis of crista galli for sex determination with a novel morphological classification on computed tomography images

Erdal Komut[1] · **Murat Golpinar**[2]

Received: 7 April 2021 / Accepted: 6 July 2021 / Published online: 10 July 2021

Abstract

Purpose This study aimed to examine the morphometry of the crista galli (CG) on paranasal sinus computed tomography (PNCT) images to develop a new approach of morphological classification with objective radiological criteria and to investigate the relationship of morphometric and morphological characteristics with gender.

Methods The height, width, and length of the CG were measured on the PNCT images of 533 subjects (266 males, 267 females). Based on the dimensions and the presence of the cavitary component of the CG, the CG was classified into three morphological types. The success of CG dimensions and new morphological classification of CG in the determination of gender was evaluated with ROC and Paired Logistic Regression analyses.

Results The morphometric cutoff values of the height, width, and length of the CG for the estimation of gender were determined as 15.15, 3.45, and 13.25 mm, respectively. CG length (accuracy 83.7%) showed more successful classification rate on gender determination as compared to height (accuracy: 81.4%), and width (accuracy 81.2%) of the CG. The presence of ossified type CG accurately identified the male sex at a rate of 88.7%, and teardrop type CG determined female sex at a rate of 82.9%. Tubular type CG identified male sex correctly at the rate of 65.8%.

Conclusion The height, length, and width measurements of CG on PNCT images and the new morphological types recommended in this study can be used in the determination of gender with high accuracy rates.

Keywords Computed tomography · Sex determination · Morphology · Classification

Introduction

Gender determination is one of the main components in the determination of identity in forensic anthropology. Osteometric and morphometric analyses are often used in gender determination [27, 29]. As the pelvic bone and skull show significant sexual dimorphism, these bone structures are accepted as the most reliable anatomical regions for gender determination [29]. In situations where bone integrity has not been preserved, knowledge of the sex characteristics of small parts of the skeleton is of great importance for gender determination [3, 19]. Morphometric approaches, which reveal sexual dimorphism in bones such as the pelvis and the skull contribute significantly to gender determination but most of the methods applied are subjective [24, 40, 42]. The use of morphological classification determined according to objective criteria in bone structures together with morphometric evaluations may present practical approaches to gender determination with high accuracy rates that do not require a high level of operator experience [46].

In forensic anthropology, various radiological imaging methods are used such as conventional radiography and computed tomography (CT) to determine gender from anatomical structures of the skull [34]. CT has become the most preferred imaging method in gender determination as complex bone structures can be visualized in detail, thereby providing reliable morphometric measurements [7, 18, 31, 38, 45]. The crista galli (CG) is an anatomical structure of ethmoid bone origin, located over the cribriform plate (CP) on the anterior side of the anterior cranial fossa [8, 30].

✉ Erdal Komut
erdalkomut@hitit.edu.tr

[1] Faculty of Medicine, Department of Radiology, Hitit University, Çorum, Turkey

[2] Faculty of Medicine, Department of Anatomy, Hitit University, Çorum, Turkey

The morphology of the CG, which may be compact bone or a pneumatized structure, varies from one individual to another. This study aimed to investigate morphometry of the CG on paranasal sinus CT (PNCT) images, to create a new approach of morphological classification with objective radiological criteria, and to investigate the relationship of morphometric and morphological characteristics of CG with gender.

Materials and methods

Approval for the study was granted by the Clinical Research Ethics Committee of Hitit University (decision no: 380 dated: 06/01/2021). The PNCT images obtained from 542 patients over 18 years 01.01.2018 and 01.01.2020 were retrieved from the hospital radiological image archiving system (PACS). The PNCT images of nine patients were excluded from the study as there was a history of trauma or surgery which affect the CG anatomy. The study included the PNCT images of 533 patients, comprising 266 males and 267 females. On the PNCT images of each patient, the height, width, and length of the CG were measured by a radiologist with 12 years of experience in neuroradiology. The morphological classification was applied on the basis of the morphometric characteristics of the CG. The presence of the pneumatization of the CG was examined on each PNCT image and the Keros classification was applied.

CT technique

The PNCT images were acquired using a 128-slice, Optima CT660 CT device (General Electric Medical Systems, Milwaukee, WI, USA). When taking the images, the patient was positioned supine and no sedation or contrast agent was used. Axial images were obtained according to following parameters: slice thickness, 1.25 mm; interval, 1.25 mm; kV, 100; mA, 120; pitch, 0.531; rotation time, 0.6 s; collimation, 20 mm; matrix, 512 × 512; FOV, 20 cm. Coronal images were obtained by reformatting the axial images with 1 mm slices thickness and 2 mm intervals, using a software program (Volume Viewer, General Electric Medical Systems, Milwaukee, WI, USA).

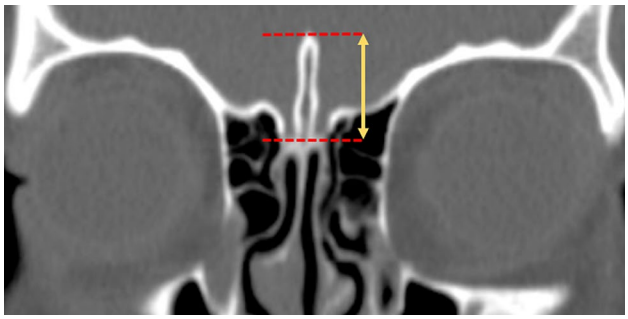

Fig. 1 Measurement of the height of the CG on coronal PNCT image

CG measurements

The height of the CG was measured on coronal slices, the width and length of the CG on axial slices. Height was measured at the highest point between the CG and the cribriform plate (CP) on coronal slices (Fig. 1). The width was recorded as the greatest transverse measurement of the CG on axial slices, taking the outer cortical borders of the CG as reference (Fig. 2). The length was calculated as the greatest anteroposterior diameter of the CG from the end of the frontal bone inner cortex on axial slices (Fig. 3).

New morphological classification for CG

The basic criteria used for morphological classification were the size measurements of the CG and the presence of a cavitary component of the CG. Accordingly, CG width more than a third greater than its height, and including a broad cavitary component were classified as Type 1, "teardrop type" on PNCT images (Fig. 4a, d). CGs with a width less than one-third of the height and containing a cavitary

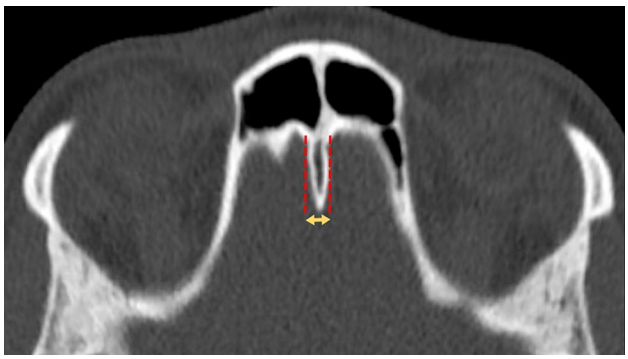

Fig. 2 Measurement of the width of the CG on axial PNCT image

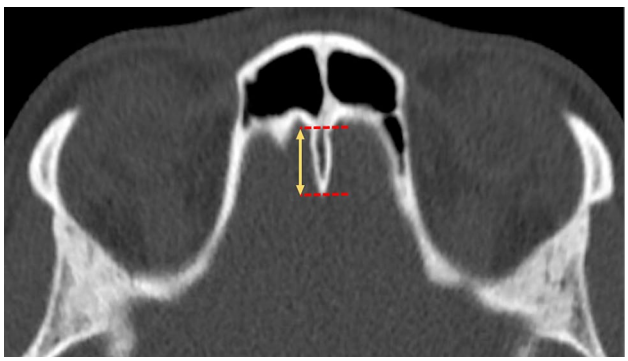

Fig. 3 Measurement of the length of the CG on axial PNCT image

component from the base to the apex were categorized as Type 2 and "tubular type" (Fig. 4b, e). CGs that were less than a third of the height in width but did not include a cavitary component were classified as Type 3, "ossified type" (Fig. 4c, f).

Keros classification

In this classification, the olfactory fossa depth is classified according to the height of the lateral lamella of the CP; type 1: 1–3 mm, type 2: 4–7 mm, and type 3: 8–12 mm [21]. In type 1, the CP and the ethmoid roof are approximately in the same plane, and in type 3, the ethmoid roof is clearly above the CP. Keros classification types on coronal PNCT images are presented in Fig. 5.

Pneumatization status

The CG was evaluated according to the presence of pneumatization (Fig. 6).

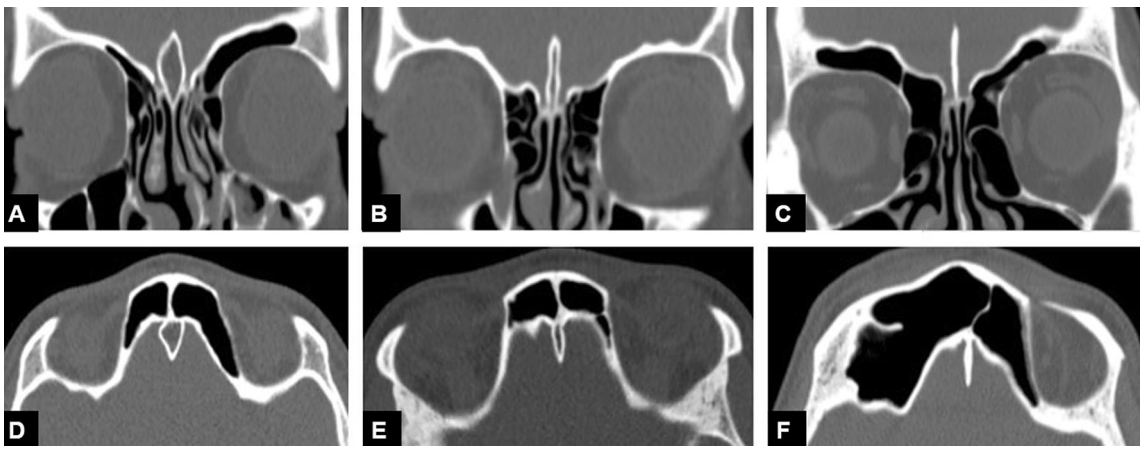

Fig. 4 New morphological classification of CG on coronal PNCT images: **A** teardrop type, **B** tubular type, and **C** ossified type. New morphological classification of CG on axial PNCT images: **D** teardrop type, **E** tubular type, and **F** ossified type

Fig. 5 Keros classification types of the CG on coronal PNCT images; **A** Keros type 1, **B** Keros type 2, **C** Keros type 3. The dotted lines indicate the upper and lower borders of the olfactory fossa. According to the new classification, **A** tubular type, **B** ossified type, **C** teardrop type are represented

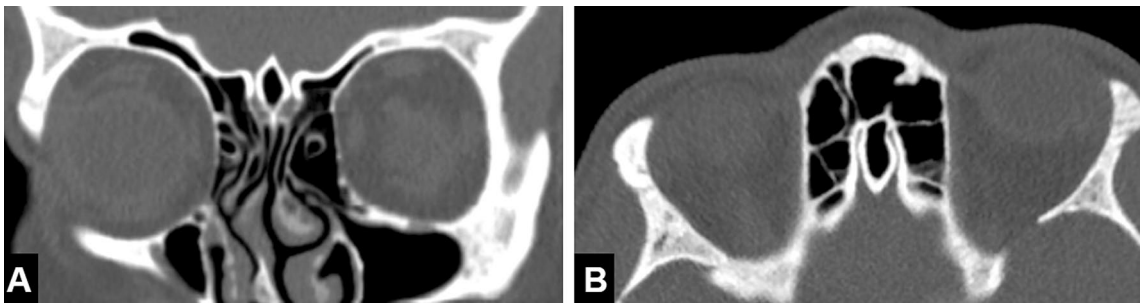

Fig. 6 A huge pneumatized crista galli on coronal (**A**) and **B** axial CT scans of the human skull

Statistical analysis

Data obtained in this study were analyzed statistically using SPSS version 22.0 (SPSS Inc., Chicago, IL, USA). In the comparison of two independent groups of numerical variables, the Student's *t* test or the Mann–Whitney *U* test was used according to the conformity of the variables to normal distribution. The χ^2 test and Fisher's Exact test were applied in the comparisons of categorical variables. The success classification rate in gender determination of the CG types with the height, width, and length values of the CG was evaluated with receiver-operating characteristic (ROC) analysis. The area under the curve (AUC) on the ROC graph was calculated with a 95% confidence interval. In the analyses, AUC of 0.9–1 was evaluated as excellent, 0.8–0.9 as good, 0.7–0.8 as moderate, 0.6–0.7 as poor, and 0.5–0.6 as a failure. The Youden Index (maximum sensitivity and specificity) was used to determine the optimal cutoff value in the ROC analysis. The success of the cutoff values was evaluated with sensitivity, specificity, positive predictive value (PPV), negative predictive value (NPV), and likelihood ratio (+). Paired Logistic Regression analysis was used to determine the effect of the CG morphometric characteristics in gender determination. For each parameter found to be statistically significant in the Logistic Regression analysis, the odds ratio (OR) and 95% CI of these were calculated. A value of $p < 0.05$ was accepted as statistically significant.

Results

The evaluation was made of the PNCT images of a total of 533 patients comprising 266 males with a mean age of 39.01 ± 15.64 years (18–85 years), and 267 females with a mean age of 38.10 ± 16.12 years (18–85 years). No statistically significant difference was determined between males and females in respect of age ($p = 0.462$). Pneumatized CG was determined in 12 (2.3%) of the 533 patients, in 4 (1.5%) males and 8 (3%) females. No statistically significant difference was determined between males and females in respect of CG pneumatization ($p = 0.245$). The mean CG height, width, and length values of all subjects are presented in Table 1. Comparison of the measurement values of the CG according to gender was presented in Fig. 7. There was a statistically significant difference between males and females in respect of CG dimensions ($p < 0.001$) (Fig. 8).

The results of the ROC analysis showing the success in gender determination of the CG height, width, and length values are presented in Table 2. In distinguishing the genders, the height and width measurements of the CG were statistically significant at a good level and the length measurements at an excellent level. The cutoff value for the height parameter was determined as 15.15, and this value showed 69.9% sensitivity for male differentiation and 92.9% specificity for female differentiation. The cutoff value for the width parameter was determined as 3.45, and this value showed 80.8% sensitivity for male differentiation and 81.6% specificity for female differentiation. The cutoff value for the length parameter was determined as 13.25, and this value showed 75.9% sensitivity for male differentiation and 90.6% specificity for female differentiation (Table 2). The ROC curves showing the predictive power of morphometric parameters in discriminating genders are shown in Fig. 8. The successful classification rates (%) of the cutoff values in gender estimation are presented in Table 3.

Table 1 Linear measurement values of the crista galli ($n = 533$)

	Mean ± SD	Median	Min–max
Height (mm)	14.22 ± 3.11	14.1	6.6–22.6
Width (mm)	3.57 ± 1.48	3.5	0.6–8.9
Length (mm)	12.78 ± 2.50	12.9	6.3–20

The comparisons of the new morphological types and Keros types of the CG according to gender are shown in Table 4. A statistically significant relationship was determined between the new morphological types of CG and gender ($p < 0.001$). No statistically significant relationship was observed between Keros classification and gender ($p = 0.158$).

The logistic regression analysis results related to the effect of morphometric characteristics of the CG in gender determination are shown in Table 5. According to the multivariate regression analysis findings, the likelihood of being male was 12.31-fold greater in those with a CG height value ≥ 15.15 mm compared to those with CG height < 15.15 mm. The likelihood of being male was 17.94-fold greater in those with a CG width value ≤ 3.45 mm compared to those with CG width > 3.45 mm. The likelihood of being male was 23.10-fold greater in those with a CG length value ≥ 13.25 mm compared to those with CG length < 13.25 mm. The odds ratios in the multivariate model were 12.31 for the measurement of height, 17.94 for width, and 23.1 for length.

Discussion

The CG is an anatomical structure localized in the midline on the cribriform plate and develops from the ethmoid bone [30]. During the embryologic period, the ethmoidal cartilage is formed by the union of a mesial mass (the mesethmoid) extending from the sphenoid to the tip of the nasal process and a pair of lateral masses that develop from the lateral nasal processes (the ectethmoid). The terminal portion of the mesial mass becomes the cartilaginous nasal septum,

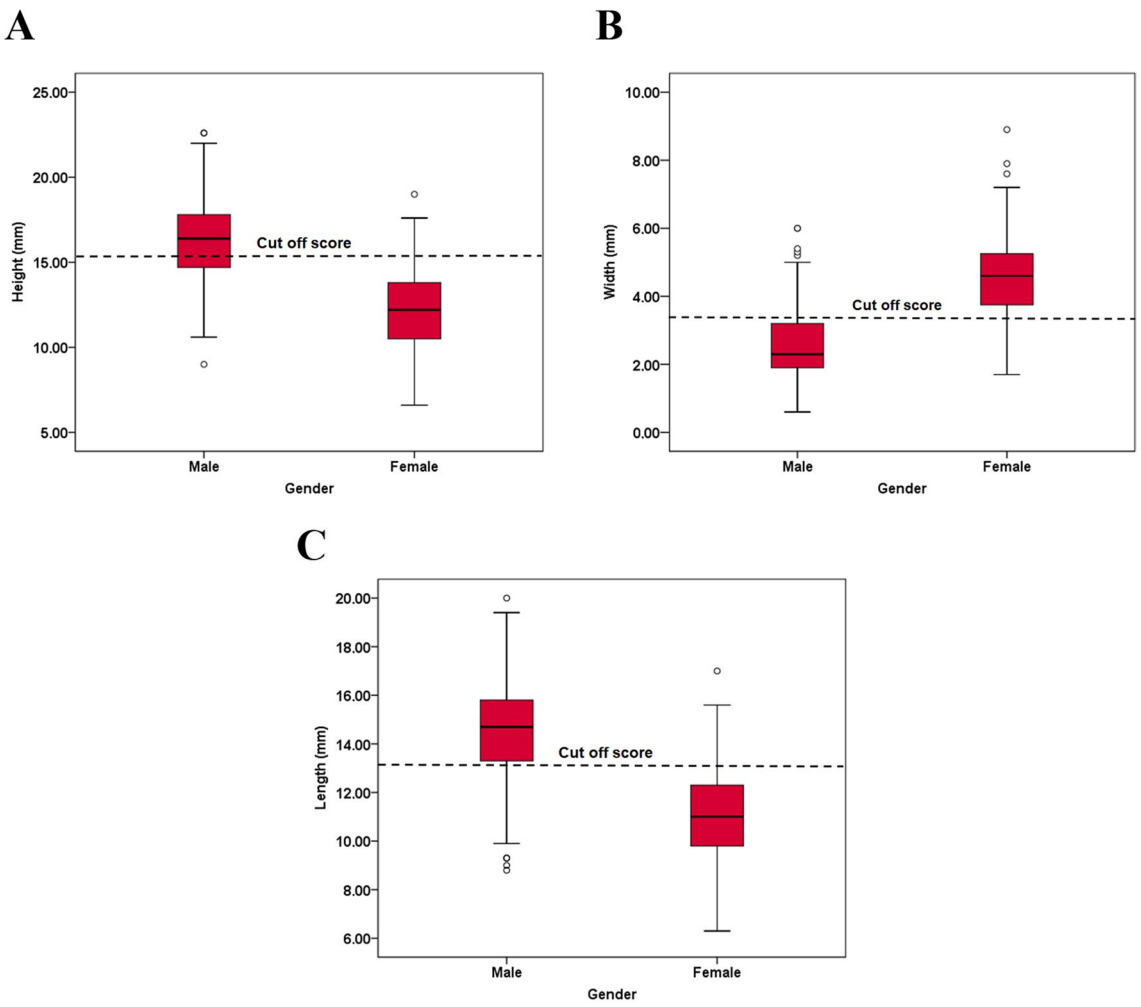

Fig. 7 Box plots for **A** height, **B** width, and **C** length measurements of CG regarding gender

and the ossification of the superior portion becomes the perpendicular plate and CG. A fair amount of ossification of the fetal CG has been reported up to week 12. However, ossification of the cartilaginous CG usually begins in the second postnatal month, gradually increases until the 14th week, afterwards slowly increases until the 24th month [9, 22, 39]. There is not any study in the literature that reports a gender difference during the embryologic development process of CG. However, a fair amount of ossification formation in fetal cartilaginous CG, up to the week 12 of intrauterine life, and the differences in the ossification rate, and termination period of ossification in the following embryological process may be related to gender characteristics.

Gender determination from skeletal remains is one of the most important steps in forensic procedures at the stage of identification [34]. The skull and the pelvis are accepted as the anatomical regions showing the most obvious sexual dimorphism [19]. The CG is a thick, smooth, triangular-shaped anatomical structure located in the midline over the cribriform plate (CP). The CG is accepted as an important anatomical landmark in anterior skull base surgery. From PNCT images, the CG can be easily evaluated morphologically and morphometrically [25].

There are a few studies in the literature which have examined the morphometry of CG. On cone-beam CT (CBCT) images of 102 skulls (76 males and 26 females), Mladina et al. reported that the height of pneumatized CG was significantly higher in females (median 14.2 mm) than in males (median 9.5 mm) [30]. In another study, Manea and Mladina examined the dimensions of pneumatized CG on the PNCT images of 196 patients with chronic rhinosinusitis. In respect of the anteroposterior diameter of the CG, there was no statistically significant difference between males (5.3–13.8 mm) and females (5.0–12.4 mm), the craniocaudal diameter of CG was slightly longer in males (5.1–12.7 mm) than females (4.7–11.2 mm) and a significant difference was determined in the latero-lateral diameter of CG in males (3.3–6.8 mm)

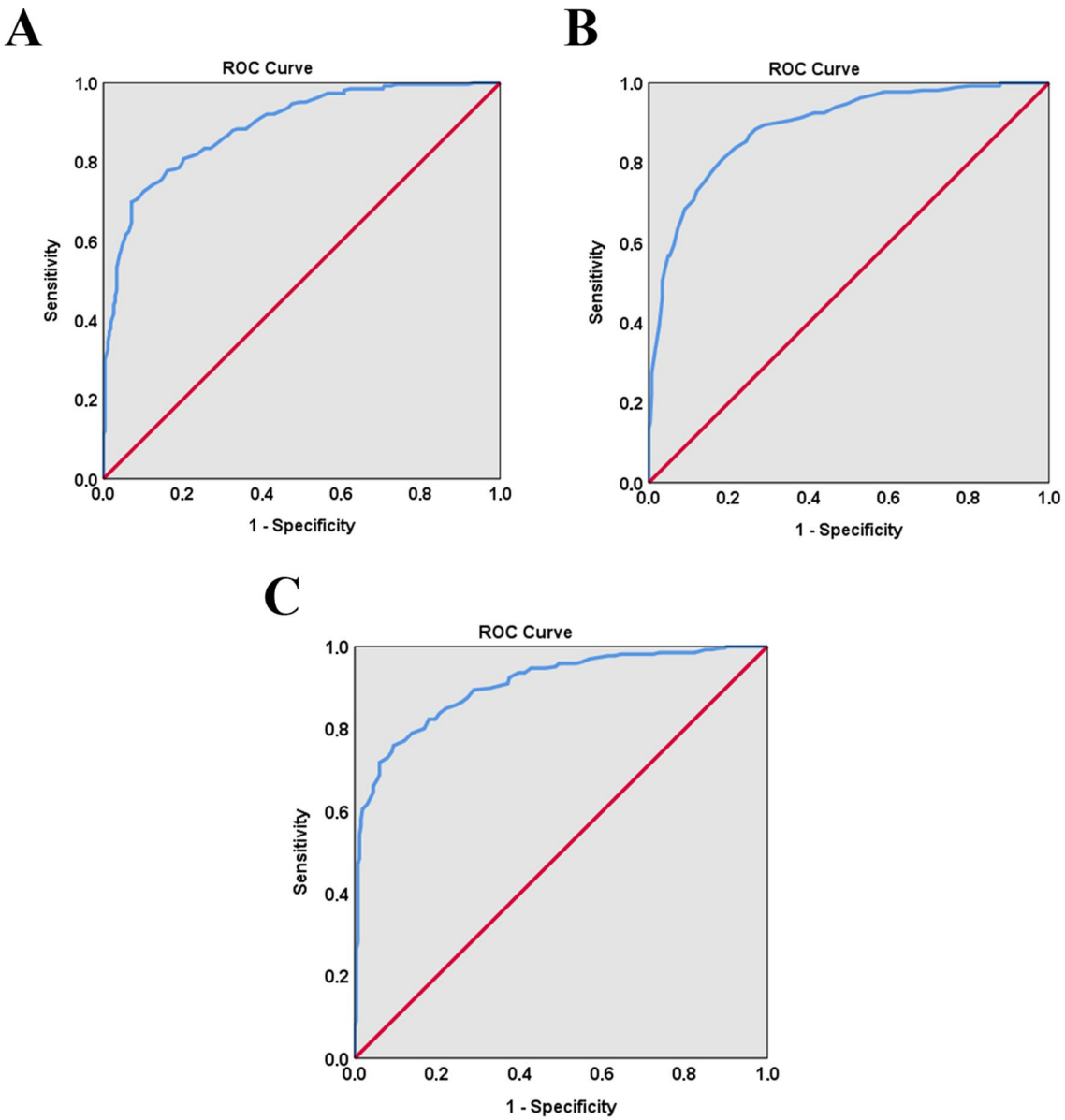

Fig. 8 ROC curves showing the predictive power of height (**A**), width (**B**), and length (**C**) measurements of CG in discriminating genders

and females (3.0–5.7 mm) [25]. In a recent study by Uçar et al., of the CBCT images of 300 healthy individuals (146 males, 154 females), the mean length and width measurements of the CG were found to be 14.05 ± 2.98 and 3.69 ± 1.53 mm, respectively, in males, and 14.02 ± 2.90 and 3.77 ± 1.43 mm in females. No significant relationship was determined between the CG length and width measurements and gender [44]. In this study, the mean CG height, width, and length values were 16.28 ± 2.41, 2.59 ± 1.00, and 14.50 ± 1.90 mm, respectively in males, and 12.17 ± 2.27, 4.55 ± 1.22, and 11.06 ± 1.73 mm, respectively, in females. In our study, unlike previous studies, dimensions of the CG exhibited sexual dimorphism. The CG was found to be significantly higher and longer in males than females, and significantly wider in females than males ($p < 0.001$).

Previous studies have reported that gender determination can be made from different anatomical structures in the skull [10, 14, 16, 36, 37]. On the other hand, there is no study in the current literature regarding the relationship between the morphometric and morphological characteristics of CG and gender. Several studies have been conducted on gender determination related to cranial anatomical structures. Sangvichien et al. examined 101 skulls and reported that with the nasion–basion length of the skull, maximum breadth of the cranium, facial length, and bizygomatic breadth of the face,

Table 2 The results of the ROC analysis showing the success in gender determination of the CG height, width, and length values

	Height	Width	Length
AUC (95% CI)	0.890 (0.863–0.916)	0.891 (0.864–0.918)	0.907 (0.882–0.932)
p value	**< 0.001**	**< 0.001**	**< 0.001**
Cutoff value (for male) (mm)	≥ 15.15	≤ 3.45	≥ 13.25
Cutoff value (for female) (mm)	< 15.15	> 3.45	< 13.25
Sensitivity (%) (male)	69.9 (64–75.3)	80.8 (75.5–85.3)	75.9 (70.3–80.9)
Specificity (%) (female)	92.9 (88.9–95.5)	81.6 (76.4–86.0)	90.6 (86.3–93.7)
PPV (%)	90.7 (85.7–94.2)	81.4 (76.1–85.8)	89.0 (84.0–92.6)
NPV (%)	75.6 (70.5–80.1)	81.0 (75.7–85.4)	79.1 (74.0–83.4)
LR+	9.83 (6.33–15.26)	4.40 (3.40–5.71)	8.11 (5.55–11.85)
Accuracy (%)	81.4	81.2	83.7

CI confidence interval, *AUC* area under the ROC curve, *PPV* positive predictive value, *NPV* negative predictive value, *LR+* positive likelihood ratio

Table 3 The successful classification rates (%) of the cutoff values in gender estimation

Parameter	Cutoff value	Gender (predicted)		Total
		Male	Female	
Height	≥ 15.15 mm (male)	186	19	205
	< 15.15 mm (female)	80	248	328
Width	≤ 3.45 mm (male)	215	49	264
	> 3.45 mm (female)	51	218	269
Length	≥ 13.25 mm (male)	202	25	227
	< 13.25 mm (female)	64	242	306
Total		266	267	533

Table 4 The comparisons of the new morphological types and Keros types of the CG according to gender

		Gender		Total	*p*
		Female	Male		
New classification					
Tear drop type	*n*	189	39	228	**< 0.001**
	%	82.9	17.1	100.0	
Tubular type	*n*	65	125	190	
	%	34.2	65.8	100.0	
Ossified type	*n*	13	102	115	
	%	11.3	88.7	100.0	
Total	*n*	267	266	533	
	%	50.1	49.9	100.0	
Keros types					
Type 1	*n*	110	119	229	0.158
	%	48.0	52.0	100.0	
Type 2	*n*	102	109	211	
	%	48.3	51.7	100.0	
Type 3	*n*	55	38	93	
	%	59.1	40.9	100.0	
Total	*n*	267	266	533	
	%	50.1	49.9	100.0	

gender could be determined with a general accuracy rate of 88.8% [37]. In a study by Paknahad et al., the relationship between gender and the maxillary sinus dimensions on 100 CBCT images was examined, and the correct predictive accuracy rate of maxillary sinus height in sex determination was reported to be 68% in males and 74% in females, with an overall accuracy of 71% [34]. In another study that obtained morphometric measurements from 438 CT images of complete and incomplete mandibula, the successful classification rates of gender determination according to 5 different bone remains scenarios were reported to vary between 76.9 and 91% for males, and 72.9–90.8% for females [43]. Nikita and Michopoulou examined the relationship between gender and the glabella, mastoid process, and external occipital protuberance in 165 skulls. The anatomical landmark showing the highest sexual dimorphism was reported to be the glabella with correct gender determination at the rate of 84.6% for males, and 79.7% for females [32]. The sexual dimorphism of the foramen magnum was examined in 72 skulls and successful classification rates of gender determination were reported as 69.6% for the sagittal diameter, 66.4% for the transverse diameter, and 70.3% for the cross-sectional area [20]. In the current study, the morphometric cutoff values for all three parameters of the CG for gender determination were 15.15 mm for CG height, 3.45 mm for CG width, and 13.25 mm for CG length. The successful classification rates of the determined cutoff values in the determination of male gender were 69.9% for CG height, 80.8% for width, and 75.9% for length. These rates for the determination of female gender were 92.9% for height, 81.6% for width, and 90.6% for length.

In this study, when the PNCT images were evaluated according to CG height ≥ 15.15 mm, width ≤ 3.45 mm, and length ≥ 13.25 mm, 186, 215, and 202 of the total 266 males, respectively, could be correctly identified. When the PNCT images were evaluated according to CG height < 15.15 mm, width > 3.45 mm, and length < 13.25 mm, 248, 218, and 242

Table 5 The logistic regression analysis results related to the effect of morphometric characteristics of the CG in gender determination

	Univariate		Multivariate	
	OR (95% CI)	*p*	OR (95% CI)	*p*
Height ≥ 15.15 mm	30.347 (17.772–51.822)	**< 0.001**	12.319 (6.030–25.167)	**< 0.001**
Width ≤ 3.45 mm	18.756 (12.140–28.976)	**< 0.001**	17.947 (9.147–35.215)	**< 0.001**
Length ≥ 13.25 mm	30.552 (18.558–50.301)	**< 0.001**	23.100 (11.351–47.010)	**< 0.001**

Nagelkerke R^2: 0.774, classification rate (accuracy): 88.6, height reference value: < 15.15 mm, length reference value: < 13.25 mm, width reference value: > 3.45 mm

OR odds ratio

of the total 267 females, respectively, could be correctly determined. Although these morphometric cutoff values could distinguish the two genders with a high accuracy rate, they were more successful in determining females as compared to males. The parameter of CG length (accuracy 83.7%) showed superior classification success in gender determination than the parameters of CG height (accuracy 81.4%) and width (accuracy 81.2%). According to the multivariate logistic regression analysis findings, when all three parameters were used together, the total classification success rate was 88.6% on gender estimation.

The vast majority of previous studies related to CG have examined the pneumatization of CG [2, 4, 11, 30, 39, 41, 44]. The rate of pneumatized CG (PCG) determined in previous studies has been reported to vary from 2.4 to 28%, and in a study conducted on skulls, the prevalence of PCG was reported to be quite different at 66% [5, 8, 30]. In the current study, PCG prevalence was 2.3%, consistent with the literature. Acar et al. [2] reported PCG incidence of 29.5% and stated that there was no association between PCG and gender. In contrast, Calışkan et al. reported prevalence of 5% and a relationship between gender and CG pneumatization [13]. In the current study, no significant relationship was determined between CG pneumatization and gender.

The Keros classification system classifies the olfactory fossa depth into three types according to the lateral lamella of the CP [21]. This classification is the classic method usually used in studies related to the CG and the olfactory regional anatomy [33]. In a study that examined the PNCT images of 150 patients (75 males, 75 females), there was reported to be a significant difference in respect of the distribution of Keros type 2 in males (22%) and females (78%) [6]. In another study, the PNCT images of 174 healthy subjects (143 females, 31 males) were evaluated and reported to be no relationship between gender and the Keros type 1 (13.79%), Keros type 2 (65.52%), and Keros type 3 (20.69%) [12]. In the current study, the distribution of CG Keros classifications in males and females was found to be 52% vs. 48% for Keros type 1, 51.7% vs. 48.3% for Keros type 2, and 40.9% vs. 59.1% for Keros type 3. No statistically significant relationship was observed between the Keros types and gender.

In contrast to the current literature, a significant relationship was determined between gender and the CG types classified as teardrop, tubular, or ossified on the coronal PNCT images. According to our results, the presence of ossified type CG could distinguish male gender at an accuracy rate of 88.7%, and the teardrop type could distinguish female gender with 82.9% accuracy. The presence of tubular type CG was able to determine the male gender with 65.8% accuracy. The morphological classification recommended for CG in this study provided the possibility of gender determination at a high rate of differentiation, similar to the osteometric approaches defined for various anatomical structures in the literature [1, 15, 17, 35].

There are two basic osteological approaches for gender determination, namely osteometric and osteomorphological. The pelvis and cranium are the two most important parts of the skeletal system that are used in gender determination with accuracy rates of 95 and 92%, respectively [23, 26]. Morphological approaches for gender determination require a high level of operator experience and are generally subjective [23]. Morphometric methods are repeatable and none of the bone structures is affected by differences in experience between operators [28].

The CG is an important anatomical structure in respect of surgical interventions to be made in this region because of its location in the anterior cranial fossa. To date, various studies have been conducted related to the morphometric properties of the CG, the presence of pneumatization, and its clinical significance. In contrast, there have been no studies on the role of the morphometric and morphological characteristics of CG in gender determination.

The results of this study demonstrated that the CG shows morphometrically sexual dimorphism. In addition, a novel morphological classification was applied with a new approach related to the morphometric measurements of CG on PNCT images. By minimizing operator error rates when making the morphological classification in this way, a new approach was developed related to objective criteria, which provides a high rate of accuracy in gender determination. This is the first CT-scanning study that has considered the relationship of CG with gender.

Nevertheless, despite the extensive sampling of the current study group, there is a need for further studies with a greater number of subjects from different Caucasian racial groups to confirm these findings of the relationship of the new morphological types of CG with gender determination.

Conclusion

The CG is a prominent anatomical structure that can be easily characterized on PNCT images. Not only because of the clinical importance of the anterior cranial fossa, but the CG is an important anatomical structure also in gender determination. The morphological types of the CG proposed in this study can be used in addition to the CG height, width, and length measurements on PNCT images in gender determination with a high rate of accuracy.

Author contributions EK and MG contributed to the study conception and design, material preparation, data collection, and analysis. The first draft of the manuscript was written by EK, and MG commented on previous versions of the manuscript. All the authors read and approved the final manuscript.

Funding The study had no funding source.

Declarations

Conflict of interest The authors declare that they have no conflict of interest.

Ethical approval This article does not contain any studies with human participants or animals performed by any of the authors.

Informed consent For this type of study, formal consent is not required.

References

1. Abdel Fatah EE, Shirley NR, Jantz RL, Mahfouz MR (2014) Improving sex estimation from crania using a novel three-dimensional quantitative method. J Forensic Sci 59:590–600. https://doi.org/10.1111/1556-4029.12379
2. Acar G, Cicekcibasi AE, Koplay M, Kelesoglu KS (2020) The relationship between the pneumatization patterns of the frontal sinus, crista galli and nasal septum: a tomography study. Turk Neurosurg 30:532–541. https://doi.org/10.5137/1019-5149.JTN.26006-19.4
3. Akhlaghi M, Bakhtavar K, Moarefdoost J, Kamali A, Rafeifar S (2016) Frontal sinus parameters in computed tomography and sex determination. Leg Med 19:22–27. https://doi.org/10.1016/j.legalmed.2016.01.008et
4. Akiyama O, Kondo A (2020) Classification of crista galli pneumatization and clinical considerations for anterior skull base surgery. J Clin Neurosci 82:225–230. https://doi.org/10.1016/j.jocn.2020.11.005
5. Al-Qudah MA (2010) Anatomical variations in sino-nasal region: a computer tomography (CT) study. J Med J 44:290–297
6. Alazzawi S, Omar R, Rahmat K, Alli K (2012) Radiological analysis of the ethmoid roof in the Malaysian population. Auris Nasus Larynx 39:393–396. https://doi.org/10.1016/j.anl.2011.10.002
7. Araki K, Maki K, Seki K, Sakamaki K, Harata Y, Sakaino R, Okano T, Seo K (2004) Characteristics of a newly developed dentomaxillofacial X-ray cone beam CT scanner (CB MercuRay^{TM}): system configuration and physical properties. Dentomaxillofac Radiol 33:51–59. https://doi.org/10.1259/dmfr/54013049
8. Bašić N, Bašić V, Jukić T, Bašić M, Jelić M, Hat J (1999) Computed tomographic imaging to determine the frequency of anatomical variations in pneumatization of the ethmoid bone. Eur Arch Otorhinolaryngol 256:69–71. https://doi.org/10.1007/s004050050118
9. Belden CJ, Mancuso AA, Kotzur IM (1997) The developing anterior skull base: CT appearance from birth to 2 years of age. AJNR Am J Neuroradiol 18:811–818
10. Choi BY, Lee KS, Han SH, Park DK, Lim NH, Koh KS, Kim HJ, Kang HS (2001) Group analysis using the metric measurements of Korean skulls. Korean J Phys Anthropol 14:207–215. https://doi.org/10.5115/acb.2014.47.3.196
11. Cobzeanu MD, Baldea V, Bâldea MC, Vonica PS, Cobzeanu BM (2014) The anatomo-radiological study of unusual extrasinusal pneumatizations: superior and supreme turbinate, crista galli process, uncinate process. Rom J Morphol Embryol 55:1099–1104
12. Costa ALF, Paixão AK, Gonçalves BC, Ogawa CM, Martinelli T, Maeda FA, Trivino T, Lopes SLPdC (2019) Cone beam computed tomography-based anatomical assessment of the olfactory fossa. Int J Dent. https://doi.org/10.1155/2019/4134260
13. Çalışkan A, Sumer AP, Bulut E (2017) Evaluation of anatomical variations of the nasal cavity and ethmoidal complex on cone-beam computed tomography. Oral Radiol 33:51–59. https://doi.org/10.5624/isd.2019.49.2.103
14. Dayal MR, Spocter MA, Bidmos MA (2008) An assessment of sex using the skull of black South Africans by discriminant function analysis. Homo 59:209–221. https://doi.org/10.1016/j.jchb.2007.01.001
15. Franklin D, Cardini A, Flavel A, Kuliukas A (2013) Estimation of sex from cranial measurements in a Western Australian population. Forensic Sci Int 229:e151-158. https://doi.org/10.1016/j.forsciint.2013.03.005
16. Franklin D, Freedman L, Milne N (2005) Sexual dimorphism and discriminant function sexing in indigenous South African crania. Homo 55:213–228. https://doi.org/10.1016/j.jchb.2004.08.001
17. Grabherr S, Cooper C, Ulrich-Bochsler S, Uldin T, Ross S, Oesterhelweg L, Bolliger S, Christe A, Schnyder P, Mangin P (2009) Estimation of sex and age of "virtual skeletons"—a feasibility study. Eur Radiol 19:419–429. https://doi.org/10.1007/s00330-008-1155-y
18. Hatcher DC, Dial C, Mayorga C (2003) Cone beam CT for pre-surgical assessment of implant sites. J Calif Dent Assoc 31:825–834
19. Iscan MY, Steyn M (2013) The human skeleton in forensic medicine. Charles C Thomas Publisher, Springfield
20. Kamath VG, Asif M, Shetty R, Avadhani R (2015) Binary logistic regression analysis of foramen magnum dimensions for sex determination. Anat Res Int. https://doi.org/10.1155/2015/459428
21. Keros P (1965) On the practical importance of differences in the level of the cribriform plate of the ethmoid. Laryngol Otol (Stuttg) 41:808–813
22. Kim JJ, Cho JH, Choi JW, Lim HW, Somng YJ, Choi SJ, Yeo NK (2012) Morphologic analysis of crista galli using computed tomography. J Rhinol 19:91–95
23. Mahakkanukrauh P, Sinthubua A, Prasitwattanaseree S, Ruengdit S, Singsuwan P, Praneatpolgrang S, Duangto P (2015) Craniometric study for sex determination in a Thai population. Anat Cell Biol 48:275. https://doi.org/10.5115/acb.2015.48.4.275

24. Mahfouz M, Badawi A, Merkl B, Fatah EEA, Pritchard E, Kesler K, Moore M, Jantz R, Jantz L (2007) Patella sex determination by 3D statistical shape models and nonlinear classifiers. Forensic Sci Int 173:161–170. https://doi.org/10.1016/j.forsciint.2007.02.024
25. Manea C, Mladina R (2016) Crista galli sinusitis—a radiological impression or a real clinical entity. Rom J Rhinol 23:167–171. https://doi.org/10.1515/rjr-2016-0019
26. Meindl RS, Lovejoy CO, Mensforth RP, Carlos LD (1985) Accuracy and direction of error in the sexing of the skeleton: implications for paleodemography. Am J Phys Anthropol 68:79–85. https://doi.org/10.1002/ajpa.1330680108
27. Memarian A, Aghakhani K, Mehrpisheh S, Fares F (2017) Gender determination from diagnostic factors on anteroposterior pelvic radiographs. J Chin Med Assoc 80:161–168. https://doi.org/10.1016/j.jcma.2016.06.009
28. Meral O, Toklu BB, Meydan R, Kaya A, Karadayı B, Acar T (2020) Sex estimation from foramen magnum parameters in adult Turkish population: a computed tomography study. Leg Med 47:101775. https://doi.org/10.1016/j.legalmed.2020.101775
29. Michiue T, Hishmat AM, Oritani S, Miyamoto K, Amin MF, Ishikawa T, Maeda H (2018) Virtual computed tomography morphometry of the patella for estimation of sex using postmortem Japanese adult data in forensic identification. Forensic Sci Int 285:e201-206. https://doi.org/10.1016/j.forsciint.2017.11.029
30. Mladina R, Antunović R, Cingi C, Muluk NB, Skitarelić N, Malić M (2017) An anatomical study of pneumatized crista galli. Neurosurg Rev 40:671–678. https://doi.org/10.1007/s10143-017-0825-0
31. Mol A, Proffit W, Cevidanes L, Bailey L (2005) Cone-beam CT image analysis of condylar changes following orthognathic surgery. Oral Surg Oral Med Oral Pathol Oral Radiol Endod 3:E26
32. Nikita E, Michopoulou E (2018) A quantitative approach for sex estimation based on cranial morphology. Am J Phys Anthropol 165:507–517. https://doi.org/10.1002/ajpa.23376
33. Paber JELB, Cabato MSD, Villarta RL, Hernandez JG (2008) Radiographic analysis of the ethmoid roof based on Keros classification among Filipinos. Philipp J Otolaryngol Head Neck Surg 23:15–19. https://doi.org/10.3241/pjohns.v23i1.763
34. Paknahad M, Shahidi S, Zarei Z (2017) Sexual dimorphism of maxillary sinus dimensions using cone-beam computed tomography. J Forensic Sci 62:395–398. https://doi.org/10.1111/1556-4029.13272
35. Ramsthaler F, Kettner M, Gehl A, Verhoff M (2010) Digital forensic osteology: morphological sexing of skeletal remains using volume-rendered cranial CT scans. Forensic Sci Int 195:148–152. https://doi.org/10.1016/j.forsciint.2009.12.010
36. Rooppakhun S, Piyasin S, Vatanapatimakul N, Kaewprom Y, Sitthiseripratip K (2011) Craniometric study of Thai skull based on three-dimensional computed tomography (CT) data. J Med Assoc Thai 93:90
37. Sangvichien S, Boonkaew K, Chuncharunee A, Komoltri C, Piyawinitwong S, Wongsawut A, Namwongsa S (2007) Sex determination in Thai skulls by using craniometry: multiple logistic regression analysis. Siriraj Med J 59:216–221
38. Scarfe WC, Farman AG, Sukovic P (2006) Clinical applications of cone-beam computed tomography in dental practice. J Can Dent Assoc 72(1):75
39. Som P, Park E, Naidich T, Lawson W (2009) Crista galli pneumatization is an extension of the adjacent frontal sinuses. AJNR Am J Neuroradiol 30:31–33. https://doi.org/10.3174/ajnr.A1291
40. Steyn M, Pretorius E, Hutten L (2004) Geometric morphometric analysis of the greater sciatic notch in South Africans. Homo 54:197–206. https://doi.org/10.1078/0018-442x-00076
41. Şahan MH, Inal M, Muluk NB, Şimşek G (2019) Cribriform plate, crista galli, olfactory fossa and septal deviation. Curr Med Imaging 15:319–325. https://doi.org/10.2174/1573405614666180314150237
42. Torimitsu S, Makino Y, Saitoh H, Sakuma A, Ishii N, Yajima D, Inokuchi G, Motomura A, Chiba F, Yamaguchi R (2017) Sex determination based on sacral and coccygeal measurements using multidetector computed tomography in a contemporary Japanese population. J Forensic Radiol Imaging 9:8–12. https://doi.org/10.1016/j.jofri.2017.01.001
43. Tunis TS, Sarig R, Cohen H, Medlej B, Peled N, May H (2017) Sex estimation using computed tomography of the mandible. Int J Legal Med 131:1691–1700. https://doi.org/10.1007/s00414-017-1554-1
44. Uçar H, Bahşi I, Orhan M, Yalçin ED (2021) The radiological evaluation of the crista galli and ıts clinical ımplications for anterior skull base surgery. J Craniofac Surg. https://doi.org/10.1097/SCS.0000000000007507
45. Urooge A, Patil BA (2017) Sexual dimorphism of maxillary sinus: a morphometric analysis using cone beam computed tomography. J Clin Diagn Res 11(3):ZC67. https://doi.org/10.7860/JCDR/2017/25159.9584
46. Zech W-D, Hatch G, Siegenthaler L, Thali MJ, Lösch S (2012) Sex determination from os sacrum by postmortem CT. Forensic Sci Int 221:39–43. https://doi.org/10.1078/0018-442x-00076